



Thickness effect on the generation of temperature and curing degree gradients in epoxy–amine thermoset systems

Cristina Monteserín¹  · Miren Blanco¹ · Jose Manuel Laza² · Estíbaliz Aranzabe¹ · Jose Luis Vilas²

Received: 29 August 2017 / Accepted: 9 February 2018 / Published online: 27 February 2018
© Akadémiai Kiadó, Budapest, Hungary 2018

Abstract

A thermo-kinetic model was employed to study the temperature and curing degree distribution in a casting part of a DGEBA–DDM system during its curing process in an oven. Initially, the curing of the DGEBA–DDM casting part system was investigated by isothermal and non-isothermal differential scanning calorimetry. A Kamal and Sourour phenomenological model expanded by a diffusion factor was proposed for modeling the curing. The proposed model fits properly the curing behavior of this system in the analyzed range of temperatures. This model enables the application within finite element analysis software for modeling the curing process of real thermosetting parts. Finite element-based program COMSOL MultiphysicsTM was used to simulate the curing process. The model fits properly the initial heating of the sample until the reaction temperature, the time position at which the temperature starts to increase due to the heat generated during epoxy–amine reaction and also the rate at which the temperature increases, but it overestimates the maximum temperatures reached in the system. Nevertheless, the proposed model is shown as a powerful tool to design optimal curing cycles for thermosetting resins avoiding temperatures closer to the degradation temperature of the system and avoiding significant temperature gradients inside the sample.

Keywords Thermosetting resin · Cure behavior · Finite element analysis (FEA) · Process monitoring

Introduction

Thermosetting materials are being widely utilized in the market as a consequence of their excellent mechanical and thermal properties, especially useful for large consumers and high technology sectors. Within this group, epoxy resins are one of the most versatile thermosetting resins widely used in different applications, such as matrices in reinforced composites, adhesives in the aerospace industry, surface coatings, etc. because of their good mechanical properties, chemical resistance and adhesive strength. In order to achieve desirable final properties, the curing

kinetics and the changes in physical states during curing must be monitored [1].

Curing schedules can not only affect the rate of reaction and the physical states during curing but also change the possible chemical reactions during curing. As a result, knowledge of curing kinetics and changes in physical states during curing is crucial for the control and optimization of final properties [2]. These transformations are highly influenced by the epoxy/hardener reaction process. Therefore, it is important to understand the curing process and its influence on the final properties of the matrix.

Because of the wrong manufacturing of polymer-matrix composite components, structural and geometrical/dimensional unconformities can be found. In most cases, these problems are caused by a wrong design of curing process in terms of thermal cycle. The geometrical and dimensional unconformities, that can compromise part assembling, show themselves in variation between real and nominal conditions, and are caused by phenomena that happen during mold heating/cooling. Structural defects, such as resin degradation and component failure, are caused by

✉ Cristina Monteserín
cristina.monteserin@tekniker.es

¹ Unidad de Química de Superficies y Nanotecnologías, Fundación Tekniker, Iñaki Goenaga 5, 20600 Eibar, Spain

² Departamento de Química Física, Facultad de Ciencia y Tecnología, Universidad del País Vasco/Euskal Herriko Unibertsitatea, Apdo. 644, 48080 Bilbao, Spain

phenomena that happen during both heating and maintenance at high temperature stage and cooling stage.

The study of processing issues related to thermosetting composites has become increasingly significant for high thickness components. Unfortunately, the process conditions for thick composites are not well known. Moreover, high thickness laminates present other problems, related to the non-uniformity of the curing process. The manufacturer's recommended curing cycle is often inadequate for thick composites, because of unfavorable effects such as large temperature gradient and heat generation. The most usual problem is a temperature overshoot due to the resin exothermic chemical reaction. The temperature distribution in the piece during the curing process is dependent on two factors, the amount of heating power provided and the quantity of heat generated by the chemical curing reaction. This last factor along with a low thermal conductivity of the resin might lead to excessively high localized temperatures that may raise to levels including material degradation [3]. On the other hand, the temperature gradient and curing degree are accentuated with the increase in the part thickness. This results in a non-homogeneous curing and an increase in the residual thermal stresses which lead to an inhomogeneity of the mechanical properties [4]. This problem becomes more important as the component thickness increases [5–9].

In consequence, it is necessary to investigate the curing process of a component in order to reach an optimum curing cycle. Such studies can be performed effectively by numerical modeling which is more general and applicable to a wider range of problems than analytical solutions. For thermosetting resins, the curing degree, the temperature, the reaction rate and the heat generation rate are mutually dependent. Therefore, the finite element modeling of the thermosetting curing process requires an iterative procedure coupling reaction kinetics with transient heat transfer analysis. As shown in literature, process modeling combined with experimental validation allows for a better understanding of curing processes and the influence of critical parameters [10–15].

According with that, this work studies the curing kinetic of an epoxy resin with DDM as a curing agent and the relationship between the curing process parameters and the final temperature and conversion degree of the thermoset networks depending on the different thicknesses. The objective of this study is to gain a fundamental understanding of the curing process to thick epoxy casting products and, in order to predict the temperature distribution and curing behavior of the thermoset, to develop a three-dimensional transient heat transfer finite element model for simulating the curing cycle for a thick epoxy cylinder part. For this, finite element-based program

COMSOL Multiphysics™ was used to simulate the curing process.

Experimental

Materials and methods

An epoxy monomer, difunctional diglycidyl ether of bisphenol A (DGEBA) supplied by Sigma-Aldrich, with an equivalent weight of 175–180 g equiv⁻¹ and a hydroxyl/epoxy ratio of 0.03, was used in this work. The curing agent, 4,4'-diaminodiphenylmethane (DDM) from Sigma-Aldrich, was a solid difunctional aromatic amine with a molecular weight of 198 g mol⁻¹ and an amine equivalent weight of 49.5 g mol⁻¹. Figure 1a, b shows the chemical structure of the epoxy resin and the amine. DGEBA epoxy resin was placed in an oven at 80 °C overnight to remove any water present. DGEBA and amine were used as received without purification. The epoxy–amine formulations were prepared stirring vigorously for 10 min at 80 °C the stoichiometric mixture among the DGEBA resin and the diamine [16, 17].

The experimental validation of the developed model has been carried out by monitoring the temperature of the DGEBA–DDM system under several curing time and temperature conditions. Different amounts of the unreacted DGEBA–DDM mixture were poured into glasses made of Pyrex with dimensions of 70 mm of height and 67 mm of diameter, resulting in 0.5 and 4 cm thickness samples. Some thermocouples, connected to a data acquisition system to monitor the temperature versus time, were placed at different locations inside the samples in order to determine the variation of temperature inside the DGEBA–DDM system during the curing process. Then, samples were put in an oven at different constant temperatures, 90 and 150 °C. So, the temperature profiles at different points inside the DGEBA–DDM mixture were recorded through the curing experiment in order to be compared with the simulated results. It was assumed that no thermal perturbation was generated by thermocouples.

The precise location of the thermocouples, shown in Fig. 2, was achieved owing to the use of a metallic or polymeric mesh as a fastener for the thermocouples. Similar results have been obtained with both types of meshes. Thermocouples were used for monitoring the systems with 0.5 and 4 cm of thickness, respectively.

The kinetic study of the DGEBA–DDM system was carried out by differential scanning calorimetry (DSC). DSC measurements were taken in a Mettler-Toledo DSC1 module in nitrogen atmosphere (50 mL min⁻¹), working with 7–10 mg samples. A fresh sample of all systems was

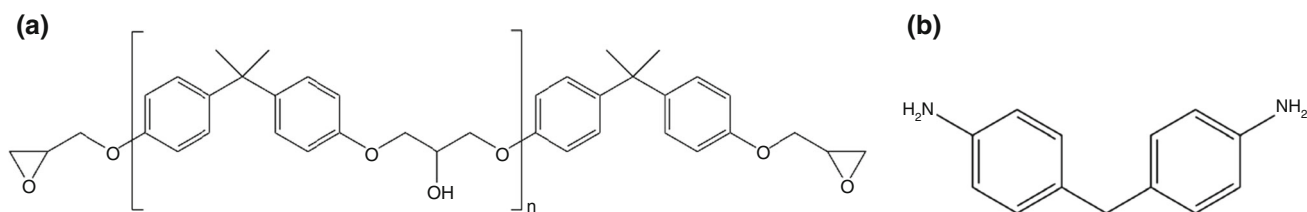


Fig. 1 Chemical structures of **a** DGEBA epoxy resin; **b** 4,4'-diaminodiphenylmethane (DDM)

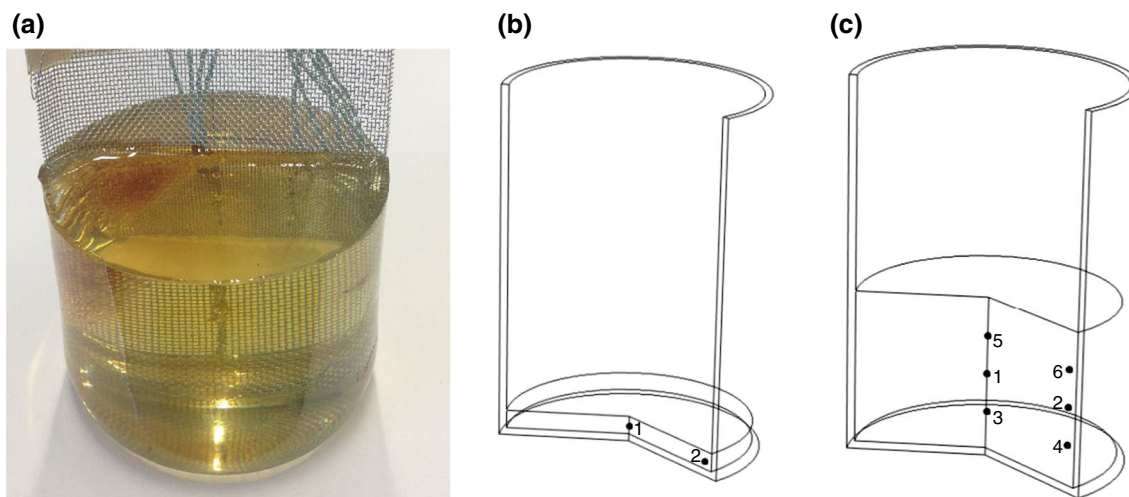


Fig. 2 **a** Device employed to fix the position of the thermocouples in the system. Thermocouples location at epoxy–amine systems with thicknesses: **b** 0.5 and **c** 4 cm

prepared before every experimental determination. Both non-isothermal and isothermal tests were carried out.

In non-isothermal tests, sample was heated from -60 to 300 °C at a constant heating rate of 10 °C min^{-1} to determine the total heat released during the dynamic curing (ΔH_T). Two consecutive dynamic scans were performed with these conditions. Dynamic DSC experiments were also performed to determine the glass transition temperature of the uncured (T_{g0}) and completely cured material ($T_{g\infty}$).

Isothermal tests were performed at temperatures ranging from 90 to 150 °C to obtain the isothermal reaction heat at each temperature (ΔH_{iso}). After each isothermal test, samples were immediately cooled to room temperature and subjected to a dynamic scan to 300 °C at 10 °C min^{-1} to measure the residual heat of the reaction (ΔH_{res}). In a second dynamic scan, the $T_{g\infty}$ was determined.

DSC analysis was also employed for the determination of the specific heat (C_p). This parameter is required for the finite element model, in order to study the heat transfer in the DGEBA–DDM system. Determination of C_p was performed using the technique TOPEM which is a temperature modulated DSC technique. In a single scan, it is possible to distinguish frequency-dependent phenomena from frequency-independent phenomena. The underlying heating

rate was 0.5 °C min^{-1} , the amplitude of the temperature pulse was ± 0.5 °C, and the switching time range to limit the duration of the pulses had the minimum of 15 s and the maximum of 30 s [18].

Results and discussion

Kinetic analysis

In Fig. 3, non-isothermal tests are represented (first and second dynamic scans). The first dynamic curve shows a change in the heat flow at low temperatures, around -16 °C, due to transition from the glassy to the liquid state of the unreacted mixture, T_{g0} . As temperature increases, the epoxy–amine reaction transforms the initial mixture in a higher molecular weight system, thus giving rise to the exothermic peak. During the reaction process, gelation and network formation occurred as well. In the second dynamic scan, the glass transition of the cured sample was determined, around 164 °C. The heat of reaction value, ΔH_T , was determined from integration of the non-isothermal DSC curve and is related to the total heat flow as it is expressed in Eq. (1) and was found to be 531.4 J g^{-1} . This value is in agreement with the reported

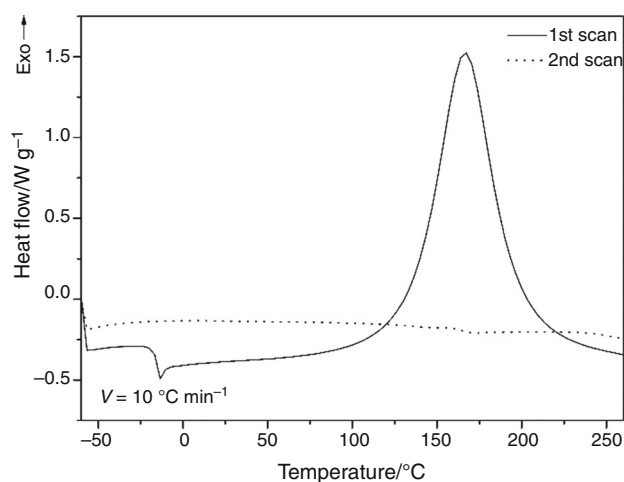


Fig. 3 Non-isothermal DSC curve for DGEBA–DDM system at a heating rate of 10 °C min^{-1}

results for the epoxy–amine reaction [19–21] and indicates the complete conversion of epoxy groups.

$$\Delta H_T = \int \frac{dQ}{dT} \frac{dT}{dt} \quad (1)$$

Polymerization kinetics of DGEBA–DDM system was studied by means of isothermal tests at different temperatures ranging from 90 to 150 °C. Figure 4a displays the isothermal DSC curves for DGEBA–DDM system at different temperatures (heat flow vs. time). These curves show a single exothermic peak for each isothermal run. The reaction rate, which is proportional to the rate of heat generation, passes through a maximum and then decreases as a function of curing time. The maximum peak value decreases and shifts to longer times with decreasing the isothermal curing temperature. Such behavior is typical of an autocatalytic reaction in which the own reaction products act as catalysts [22].

The heat released during the isothermal test (ΔH_{iso}) is the area integrated below the resulting curve spanning from time zero (t_0) to the end of isothermal stage (t_{end}), Eq. (2).

$$\Delta H_{\text{iso}} = \int \frac{dQ}{dt} \quad (2)$$

Figure 4b, c displays the subsequent non-isothermal DSC scans. As expected, Fig. 4b shows that the residual heat of reaction decreases with an increase in isothermal curing temperature. The decrease in residual heat of reaction and increase in T_g shows the progress of curing reaction with temperature. Fig. 4c shows the glass transition temperature of the completely cured material.

Table 1 collects all the values of reaction heat determined from the isothermal DSC tests and the subsequent dynamic scans: the isothermal heat of reaction at a specific temperature (ΔH_{iso}), the residual heat of reaction (ΔH_{res}) and the total heat of reaction ($\Delta H_{\text{tot}} = \Delta H_{\text{iso}} + \Delta H_{\text{res}}$). In

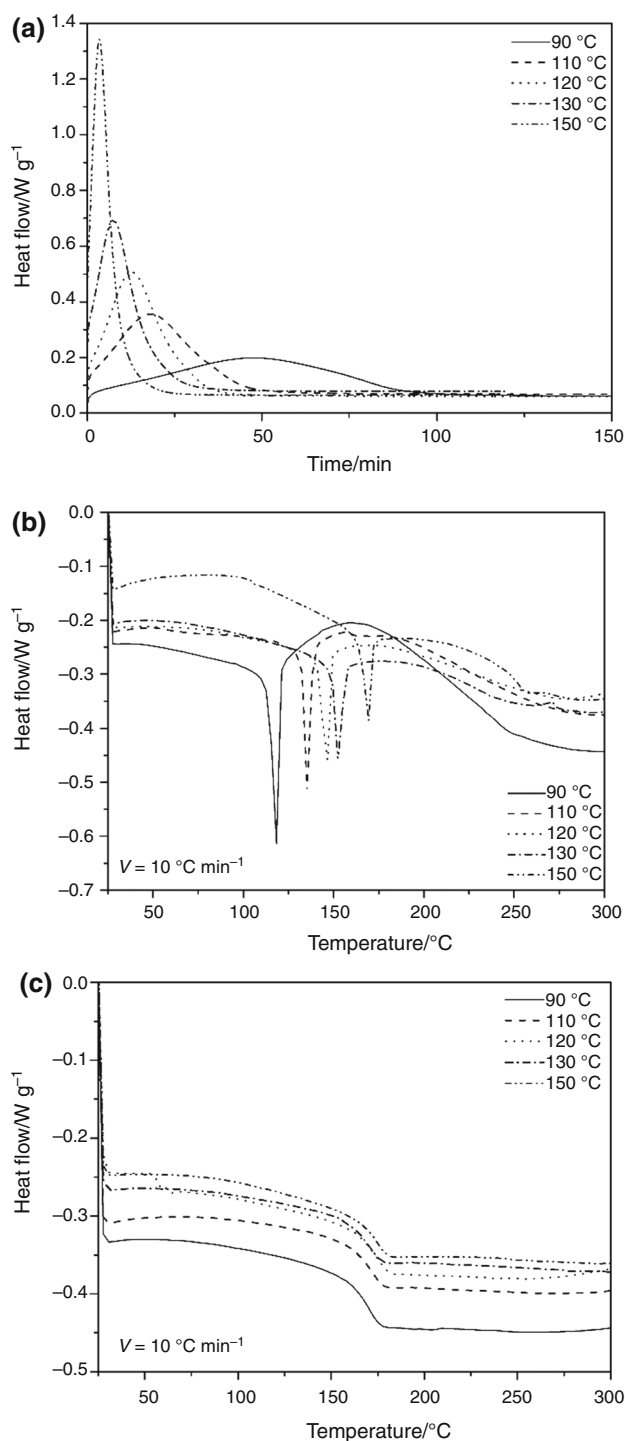


Fig. 4 a Isothermal DSC curves for DGEBA–DDM system at different temperatures, b first and c second subsequent non-isothermal DSC curves

addition, the $T_{g\infty}$ values of the cured samples are also collected in Table 1. It can be observed that as the temperature increases, the isothermal heat generated in the reaction systematically increases, whereas the residual heat of reaction decreases. Thereby, the total heat of reaction

Table 1 Results of isothermal DSC measurements and subsequent dynamic scans

$T/^\circ\text{C}$	$\Delta H_{\text{iso}}/\text{J g}^{-1}$	$\Delta H_{\text{res}}/\text{J g}^{-1}$	$\Delta H_{\text{tot}}/\text{J g}^{-1}$	$Tg_{\alpha}/^\circ\text{C}$
90	459	70	530	169
110	490	37	526	170
120	508	22	529	172
130	509	13	522	169
150	513	12	525	172

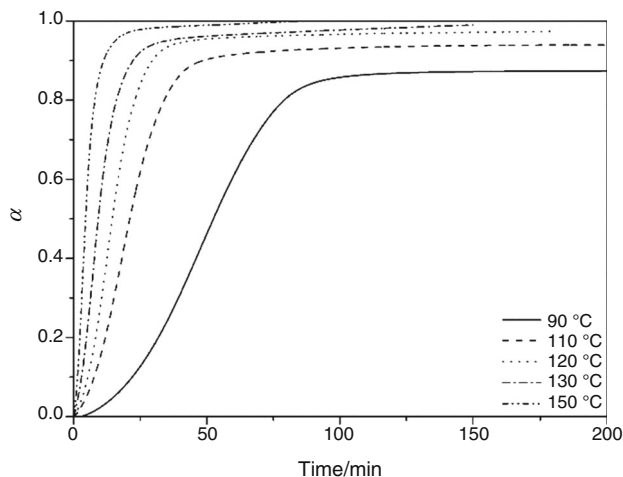
remains practically constant in the range of values reported in the literature [23, 24]. The total heat of reaction is a little smaller than the dynamically found (531.4 J g^{-1}), due to the heat losses at the beginning of the isothermal curing.

The curing process of a thermosetting resin results in conversion of a low molecular weight monomers or prepolymers into a highly crosslinked, three-dimensional macromolecular structure. The curing degree, α , is generally used to indicate the extent of the resin chemical reaction. α is proportional to the amount of heat given off by bond formation and is usually defined as shown in Eq. 3:

$$\alpha = \frac{\Delta H_{\text{iso}}}{\Delta H_{\text{tot}}} \quad (3)$$

For an uncured resin $\alpha = 0$, whereas for a completely cured resin $\alpha = 1$.

Typical plots of α versus time are reported in Fig. 5, whose shape clearly evidences the autocatalytic nature of the process. At each specific temperature, it can be observed that α increases rapidly with time. For higher α values, the increase becomes slower, to level off to a limiting conversion $\alpha(T)$. Increasing the curing


Fig. 5 Conversion versus time profiles for DGEBA–DDM system at different temperatures

temperature, the conversion increases faster and leads to higher $\alpha(T)$.

Kinetic model development

Once the curing behavior of the resin has been examined by DSC, it is important to find a simple and accurate kinetic model to describe the curing behavior. A variety of kinetic models have been developed to relate the reaction rate and curing degree. Curing kinetics models can be classified into two categories, phenomenological models and mechanistic models. Mechanistic models consider the individual chemical reaction taking place in the thermoset system, so they are difficult to handle from the modeling point of view. However, phenomenological or semi-empirical models do not require a deep knowledge of the reaction mechanism, so they are the most common models to describe thermoset curing reactions [23, 25]. The phenomenological Kamal and Sourour model of curing kinetics seems to be the model most widely used in the literature for epoxy systems [24, 26]. This model, expressed by Eq. (4), accounts for an autocatalytic and non-autocatalytic reaction in which the initial reaction rate is not zero.

$$d\alpha/dt = (k_1 + k_2\alpha^m)(1 - \alpha)^n \quad (4)$$

where α is the curing degree or conversion, $d\alpha/dt$ the rate of conversion of epoxy groups at a given time t , k_1 and k_2 are rate constants, m and n are the kinetic exponents of the reaction, and $(m + n)$ gives the overall order of the curing reaction. k_1 describes the rate constant of the reaction of partial order n catalyzed by an accelerator (non-autocatalytic), k_2 is the rate constant of the autocatalytic reaction of partial order m . The kinetic constants k_1 and k_2 are temperature dependent, usually assumed to follow an Arrhenius relation according to Eq. (5),

$$k_i = A_i \exp\left(-\frac{E_i}{RT}\right) \quad (5)$$

where k_i and E_i are the rate constant and the activation energy, respectively; A_i is the frequency factor which is a constant, R is the universal gas constant ($8.314 \text{ J mol}^{-1} \text{ K}^{-1}$), and T is the absolute temperature. The kinetic parameters of the curing reaction are obtained by fitting the data obtained from the DSC measurements to the phenomenological reaction models. Thus, the kinetic model discussed above allows calculation of E_i , using linear regression on data obtained at different temperatures.

The fitting curves from the experimental data to the autocatalytic Kamal and Sourour kinetic model are shown in Fig. 6, where the dots are the experimental rates and the full lines are the fitting curves. Clearly, the experimental curves accord well with the fitting ones at the early stage,

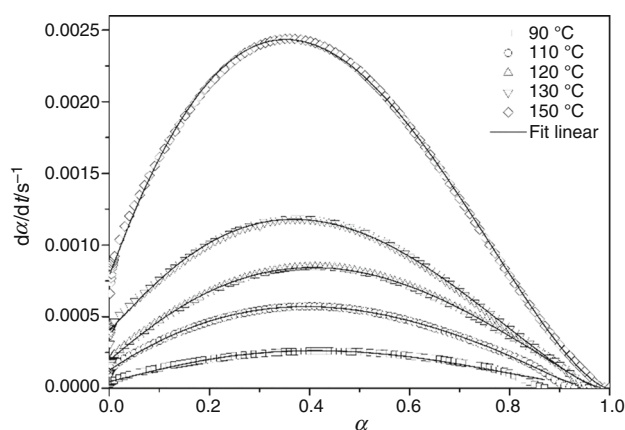


Fig. 6 Isothermal conversion rate versus conversion profiles for DGEBA–DDM system obtained at different temperatures

but at high conversion ($\alpha > 0.8$), a discrepancy appears because of the diffusion-controlled reaction kinetics. Increasing the isothermal curing temperature delays this deviation to higher conversions, because of the improved chain mobility in the network at high temperatures.

Kinetic parameters of the Kamal and Sourour model (k_1 , k_2 , m and n) are summarized in Table 2. They were determined fitting the experimental data from each isothermal curve by means of Levenberg–Marquardt non-linear regression analysis to the Kamal and Sourour equation. As shown in Table 2, k_2 is much greater than k_1 , indicating that the autocatalytic reaction is much faster than the non-autocatalytic reaction. The orders of reaction, m and n , change slightly with temperature, reflecting the complex nature of the reaction mechanism, but their sum is in the range 2.5–3 which is in a good agreement with the literature for epoxies [27].

Considering the Arrhenius law, Eq. (5), and plotting $\text{Ln } k_1$ and $\text{Ln } k_2$ versus $1/T$ (Fig. 7) can be calculated the activation energy for the non-autocatalytic reaction, E_1 , and for the autocatalytic reaction, E_2 . Table 3 also shows the constants A_1 and A_2 , and the average values for the kinetic exponents of the reaction (n and m) and the overall order of the curing reaction ($n + m$). These data indicate

Table 2 Kinetic rate parameters obtained with the applied Kamal and Sourour model for the DGEBA–DDM system studied at different temperatures

$T/^\circ\text{C}$	k_1/s^{-1}	k_2/s^{-1}	m	n	$n + m$	R^2
90	5.0×10^{-5}	1.5×10^{-3}	1.15	1.51	2.66	0.97
110	1.3×10^{-4}	3.0×10^{-3}	1.08	1.49	2.57	0.99
120	2.0×10^{-4}	4.1×10^{-3}	1.08	1.39	2.47	0.99
130	4.1×10^{-4}	6.0×10^{-3}	1.08	1.56	2.64	0.99
150	7.9×10^{-4}	1.2×10^{-2}	1.03	1.58	2.61	0.99

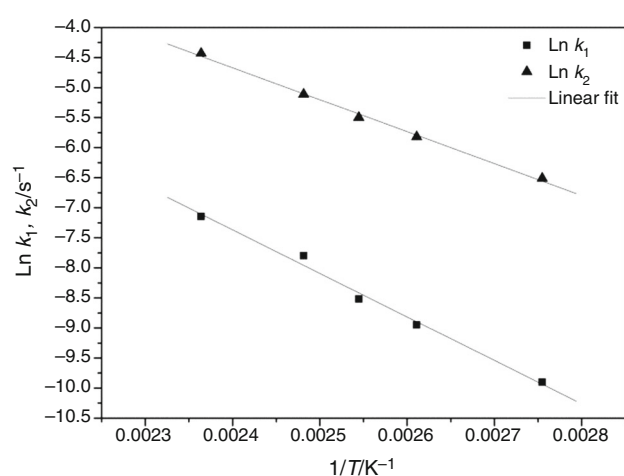


Fig. 7 Arrhenius-type plots of rate constants $\text{Ln } k_1$ and $\text{Ln } k_2$. The solid lines represent the linear fit

that for the same reaction system, E_2 is somewhat lower than E_1 , in good agreement with values obtained by other authors for similar systems [28, 29].

The obtained results indicate that the Kamal and Sourour kinetic model allows obtaining a good fit to experimental data in the first stages of reaction, but deviations are observed at high levels of conversion due to the diffusion-controlled reaction kinetics. In this region, the glass transition temperature of the reactive system reaches the curing temperature and the resin passes from a rubbery state to a glassy state. At this stage, the reaction rate undergoes a decrease and the viscosity increases, so the mobility of the unreacted groups is hindered and the rate of conversion is controlled by diffusion rather than chemical factors. The reaction rate decreases with the increase in conversion and approaches to zero at the end of the reaction, as the glass transition temperature T_g increases. To consider the diffusion effect, Chern and Phoehlein proposed another definition of the reaction rate by adding a diffusion factor to the kinetic model [30], which is defined in Eq. (6).

$$\left[\frac{d\alpha}{dt} \right]_{\text{Diffusion}} = f(\alpha) \frac{1}{1 + \exp[C(\alpha - \alpha_c)]} \quad (6)$$

where $1/(1 + \exp[C(\alpha - \alpha_c)])$ is the diffusion control factor, C is an empiric parameter which is temperature dependent, α_c is the critical curing degree at which diffusion initiates (the value of the conversion at rate of conversion $d\alpha/dt = f(\alpha)/2$, and $f(\alpha)$ is the kinetic expression of the previous Kamal and Sourour model expressed in Eq. 5. For $\alpha < \alpha_c$, the expression $(1/1 + \exp[C(\alpha - \alpha_c)])$ tends to unity and the kinetic reaction is chemically controlled. When the conversion reaches its critical value, α_c , $(1/1 + \exp[C(\alpha - \alpha_c)]) = 0.5$. For $\alpha > \alpha_c$, $(1/1 + \exp[C(\alpha - \alpha_c)])$ tends to zero and the reaction rate dramatically decreases and finally stops.

Table 3 Kinetic rate parameters obtained with the applied Kamal and Sourour model for the DGEBA–DDM system

A_1/s^{-1}	A_2/s^{-1}	$E_1/kJ\ mol^{-1}$	$E_2/kJ\ mol^{-1}$	m	n	$n + m$
2.39×10^4	3.25×10^3	60.2	44.2	1.08	1.51	2.59

Figure 8 shows the correlation between experimental kinetic data and the simulated curve based on the Kamal and Sourour model with and without including the diffusion-controlled term for the system DGEBA–DDM cured at 90 °C. It is interesting to note that the theoretical prediction of the Kamal and Sourour model fails at conversions close to gelation area, which in a bifunctional epoxy–tetrafunctional amine system is around $\alpha = 0.5$. After gelation, the viscosity of the system is increasing and, therefore the kinetics, instead of being controlled by the chemical reactivity of the functional groups, becomes more and more controlled by the diffusion of these groups in the vicinity of the glassy state. On the contrary, when the diffusion factor is considered in the kinetic model (Chern and Phoehlein kinetic model), the experimental results were accurately simulated until high conversion values.

Table 4 summarizes the kinetic parameters of the Kamal and Sourour model expanded by a diffusion factor, determined fitting the experimental data from each isothermal curve in a similar way as it explained above. Once again, k_2 is much greater than k_1 , indicating that the autocatalytic reaction is much faster than the non-autocatalytic reaction. Moreover, the order reactions, m and n , practically remain constant with the temperature, being slightly lower than values obtained applying the Kamal and Sourour model without considering the diffusion factor. Thereby, the overall order of the curing reaction ($n + m$) is also lower. Finally, it can be observed in Table 4 that the critical curing degree at which diffusion initiates (α_c) increases

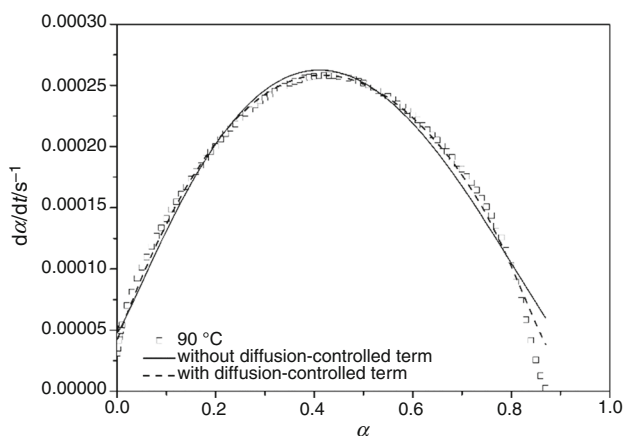


Fig. 8 Isothermal conversion rate versus conversion profiles for DGEBA–DDM system cured at 90 °C. The lines represent the theoretical prediction of the Kamal and Sourour model

with temperature, that is, the diffusion factor is less important when the temperature rises. This increase with the temperature could be fitted by a linear function [27]. On the other hand, the diffusion control factor is higher at lower temperatures; hence, parameter C was logically found as a decreasing function of temperature.

The activation energies for the non-autocatalytic reaction, E_1 , and for the autocatalytic reaction, E_2 , were determined by considering that k_1 and k_2 follow the Arrhenius law (Fig. 9). The obtained values for E_1 and E_2 were 64 and 45.8 kJ mol⁻¹, respectively, Table 5. These data indicate that for the same reaction system, E_2 is somewhat lower than E_1 , in good agreement with values obtained by other authors for similar systems [11, 12]. The activation energies found considering the diffusion process are slightly higher than ones obtained when the diffusion process is not considered.

Finite element model

For a fluid, the heat transfer equation in terms of temperature is based on Fourier's heat conduction equation the transient heat transfer and an internal heat generation term, and can be described by Eq. (7).

$$\rho C_p \frac{\partial T}{\partial t} + \rho C_p u \cdot \nabla T = \nabla \cdot (k \nabla T) + Q \quad (7)$$

where ρ , C_p and k are the density, the specific heat capacity and the thermal conductivity of the composite material, respectively, u is the velocity vector, T is the absolute temperature, and Q is the heat source. This equation assumes that mass is always conserved.

For a thermoset resin, the heat generation source in Eq. (7) represents the exothermic effect of the curing reaction. This term is directly related to the curing rate by Eq. (8).

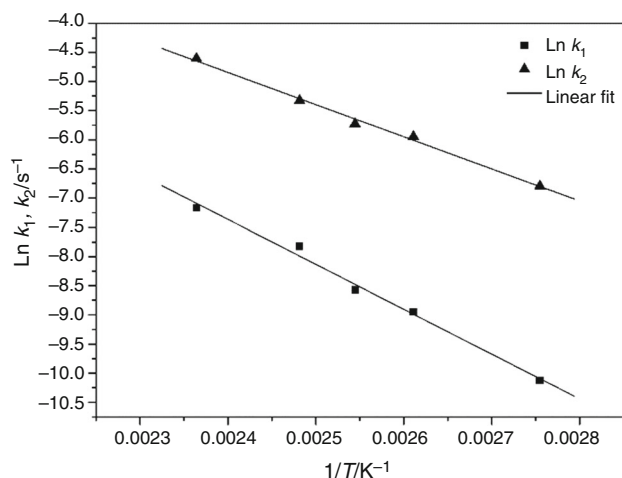
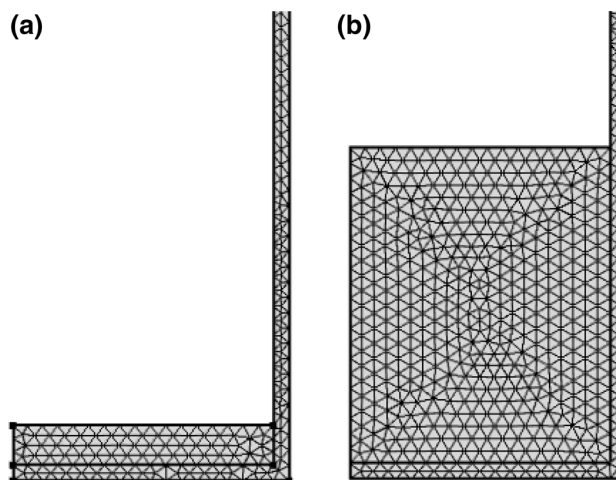
$$Q = v_r \rho_r \Delta H_T \frac{d\alpha}{dt} \quad (8)$$

where α is the curing degree, ρ_r is the density of the resin, v_r is the resin volume fraction which in this case is 1, and $d\alpha/dt$ is the reaction curing rate. The $d\alpha/dt$ term has been previously defined in “Kinetic model development” section.

In order to analyze the heat transfer in the DGEBA–DDM system taking into account the effect of the exothermic reaction, a numerical procedure was proposed

Table 4 Kinetic rate parameters obtained with the applied Kamal and Sourour model expanded by a diffusion factor for the DGEBA–DDM system studied at different temperatures

$T/^\circ\text{C}$	α_c	k_1/s^{-1}	k_2/s^{-1}	m	n	C	$n + m$	R^2
90	0.87	4.0×10^{-5}	1.1×10^{-3}	0.99	1.27	23.8	2.26	0.99
110	0.93	1.3×10^{-4}	2.6×10^{-3}	1.01	1.39	24.6	2.40	0.99
120	0.97	1.9×10^{-4}	3.3×10^{-3}	0.98	1.09	5.84	2.07	0.99
130	0.98	4.0×10^{-4}	4.8×10^{-3}	1.01	1.27	5.60	2.28	0.99
150	1.00	7.7×10^{-4}	1.0×10^{-2}	0.96	1.31	5.08	2.27	0.99

**Fig. 9** Arrhenius-type plots of rate constants $\text{Ln } k_1$ and $\text{Ln } k_2$. The solid lines represent the linear fit**Fig. 10** Mesh and boundary conditions for the system with a thickness of **a** 0.5 cm and **b** 4 cm**Table 5** Kinetic rate parameters obtained with the applied Kamal and Sourour model expanded by a diffusion factor for the DGEBA–DDM system

A_1/s^{-1}	A_2/s^{-1}	$E_1/\text{kJ mol}^{-1}$	$E_2/\text{kJ mol}^{-1}$	m	n	$n + m$
6.63×10^4	4.37×10^3	64.0	45.8	0.99	1.26	2.25

in which a finite element-based program COMSOL MultiphysicsTM was employed to perform transient heat transfer analysis and to simulate the curing reaction of the thermoset system. A two-dimensional finite element analysis on an axisymmetric slice was performed.

First, the transient heat transfer model is defined in the heat transfer module of the software to obtain the temperature profile. Then, a general form equation is considered separately in the partial differential equation (PDE) module to evaluate the curing kinetics and curing degree reached in each element. The transient simulations were conducted with a direct PARDISO solver and backward differentiation formula (BDF). A step-time size of 1 s was used to predict accurate results. Due to the axial symmetry, the final geometry has 2 domains, 9 boundaries, and 8 vertices, and the mesh was performed using the predefined extra-fine option resulting in 435 domain elements and 157 boundary elements for the system with a thickness of 0.5 cm (Fig. 10a) and 1197 domain elements and 175

boundary elements for the system with a thickness of 4 cm (Fig. 10b).

In the model, a convective boundary condition on the faces of the glass exposed to the oven environment modeled the thermal loading. The boundary condition was set as free external convection and described by Eq. (9).

$$-n \cdot (-k \cdot \nabla T) = h(T_{\text{ext}} - T) \quad (9)$$

where n is the normal vector of the boundary, h is the free convection coefficient to air defined by $h = h_{\text{air}}(L, p_A, T_{\text{ext}})$, being L the wall height (9.7 cm), p_A absolute pressure (1 atm), and T_{ext} the temperature of the heater (90 or 150 °C).

For solving the analysis, the thermo-physical properties of the thermoset system and the glass are required. For the Pyrex glass, the main parameters are $C_p = 850 \text{ J kg}^{-1} \text{ K}^{-1}$, $k = 1.4 \text{ W m}^{-1} \text{ K}^{-1}$ and $\rho = 2.23 \text{ kg m}^{-3}$. For the DGEBA–DDM system, constant values for the thermo-physical properties at room temperature were assumed. The

density was taken from the DGEBA resin, with a value of 1168 kg m^{-3} , and for the thermal conductivity, a constant theoretical value of $0.2 \text{ W m}^{-1} \text{ K}^{-1}$ was considered since it appears that the slight change of thermal conductivity with temperature has negligible effects on the thermal model [31–33]. Concerning the C_p , the variation of the heat capacity with the conversion degree and the reaction temperature was obtained by DSC and included in the thermal model [34, 35].

In the modeling, it was assumed that no resin flow or thickness reduction occurs during the curing process. The heat equation can be solved considering that at $t = 0$, $T = T_0$ and $\alpha = \alpha_0$ ($\alpha_0 = 0$), where T_0 and α are the initial temperature and curing degree of the material, respectively.

For the validation of the model and for testing its reliability, the curing of the DGEBA–DDM system was carried out into Pyrex glasses in an oven at constant temperature, as it is described in the experimental part, and temperature profiles inside the system were recorded throughout the experiment and compared with the numerical results provided by the finite element model. Figure 2 shows the thermocouples location for the experiments at the different thicknesses.

Different experiments were performed with constant oven temperatures of 90 and 150 °C and epoxy–amine systems with different thicknesses (0.5 and 4 cm). Figure 11 shows the temperature profiles at different points of the middle thickness section in the system with a thickness of 0.5 and 4 cm at 90 and 150 °C obtained through the experiment and compared with the numerical simulation results.

The samples were introduced in the oven at temperatures around 60 °C, and they were monitored for 250 min. Both experimental and modeled data showed an increase in the samples initial temperatures until the temperature of the test was reached. The model fitted quite properly this first heating step. Thereafter, the samples temperatures increase faster, as a consequence of the heat generated inside the samples due to the epoxy–amine reaction, until the system reached a maximum temperature. As it was expected, for systems cured at lower temperatures, these maximum temperatures are lower and were achieved at longer times than for systems cured at higher temperatures. For all the analyzed conditions, the time position of the peak predicted by the model correlated properly with the experimental data, and also the rate at which the temperature increase (slope of the profile). However, the model predicted temperatures higher than the temperatures measured by the thermocouples because the model overestimated the heat generated by the resin during curing. This could be due to a heat dissipation problem, not considered in the model. The difference is higher than the ones reported in bibliography [15, 33]. This could be due to

the high curing temperatures employed in this work and the high heat of reaction for DGEBA–DDM system that implies a generation of a high quantity of heat in a short period of time.

Concerning the thickness effect on the temperature response of the material, it can be observed that an increase in the thickness generates an increase in the maximum temperature reached in both points of the system for all the studied curing temperatures. This effect is even more significant in the center of the material, so the curing degree evolves differently. In a system cured at 150 °C, for a thickness of 0.5 cm, the maximum peak temperature in the center of the piece (thermocouple 1) was around 235 °C, whereas this peak was of 283 °C for a thickness of 40 mm (thermocouple 1). This fact highlights the necessity of an accurate thermo-chemical model to design the curing in order to avoid the use of temperatures close to the degradation temperature of the material.

For all the analyzed condition, the temperatures reached at the central point of the system and at the edge were different in both experimental and modeled data. The temperature at the edge was lower because the heat generated in the sample was dissipated faster. The differences between the center and the edge temperatures were even higher than 55 °C, for experimental and modeled data, depending of the curing temperature and thickness of the sample.

The temperature gradient across the thickness of the sample has also been analyzed. Figure 12 shows the experimental and modeled temperature profiles at different points of the middle position (points 1, 3 and 5) and of the edge position (points 2, 4 and 6) at 90 and 150 °C for the systems with a thickness of 4 cm. It can be observed that experimental temperature is quite similar in the central area and in the edge. Only a small reduction in the experimental maximum temperature for the points closer to the glass is observed, due to some insulating effect of the glass and to the heat dissipation contribution.

The proposed model can help to analyze the temperature gradient and the curing degree generated in a specific system. Figures 13 and 14 show the temperature and curing degree distribution provided by the model inside the epoxy–amine system cured at 90 °C after different curing times for the system with a thickness of 0.5 cm (Figs. 13a, 14a) and 4 cm (Figs. 13b, 14b).

In the system with 0.5 cm thickness, the heating started as a consequence of the heat in the oven and this heat propagated from the external part until the center of the system in a fast way, as the volume of resin to be heated is small. A slight reaction is caused by this temperature, and the curing degree slightly increased. The temperature in the center of the system started to increase fast due to the heat generated by the epoxy–amine reaction. This increase is

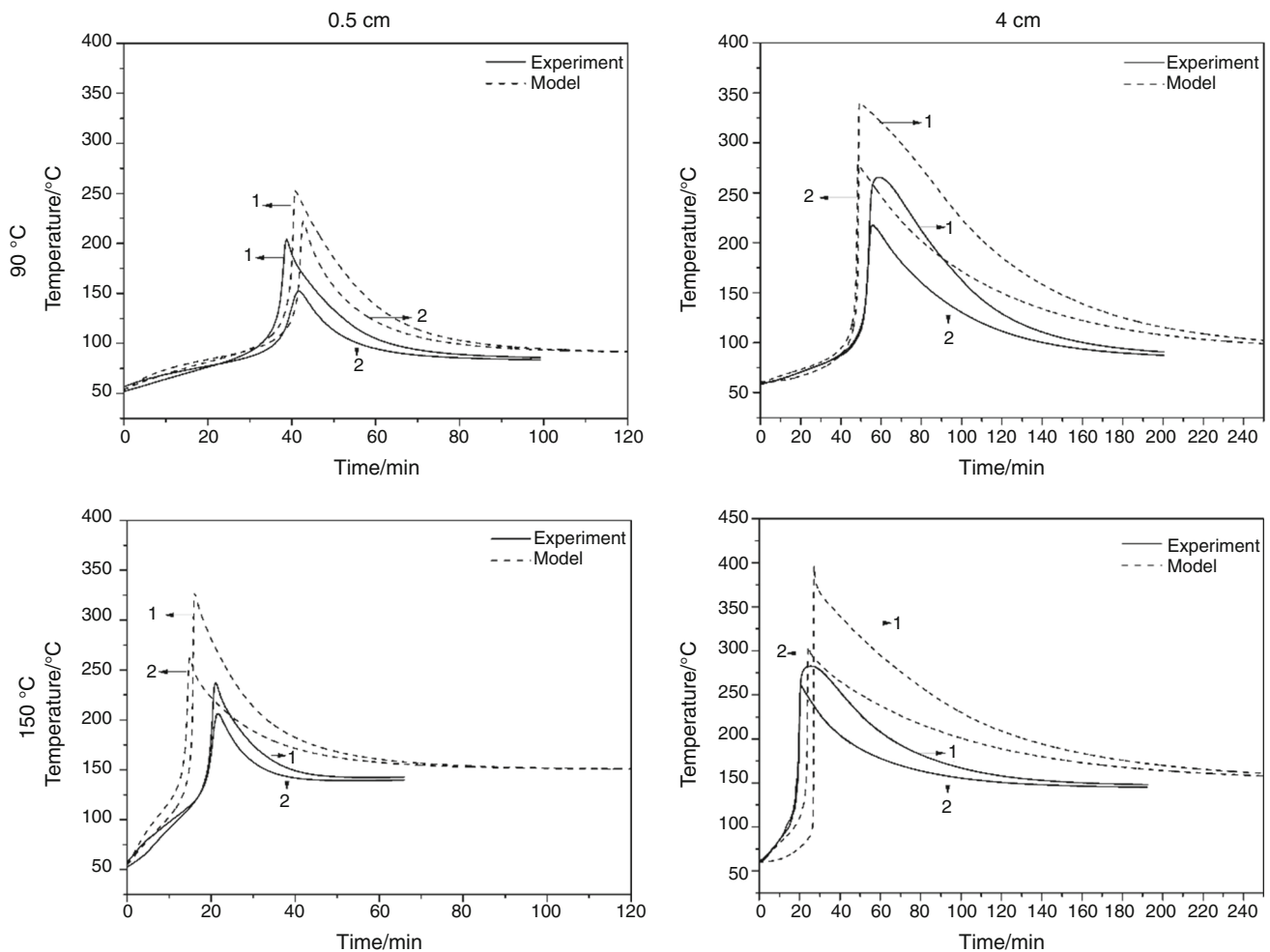


Fig. 11 Comparison of experimental and predicted temperature profiles of the DGEBA–DDM system at curing temperatures of 90 and 150 °C and at two different locations (1) center and (2) edge of the middle thickness section for the systems with thicknesses 0.5 and 4 cm

higher in the center because the temperature is enhanced by the contribution of the heat generated by the resin around the material in the center and due to dissipation problems, which are more important in the center, as it is the area farthest from the glass. At this point, the crosslinking occurs at a faster rate leading to a non-uniform curing degree [13–15, 33]. With the time evolution, the reaction ends, the system achieved a high curing degree, and no more heat is generated. Then, the temperature decreased. The temperature of the material in contact with the glass decreased faster and the temperature in the center dissipated more slowly. Finally, as it can be expected, the temperature tends to be the one in the oven. A full curing degree is achieved in the sample.

In the system with 4 cm thickness, also the heat in the oven started heating the resin from the outer part of the glass, but the heating is slower as the amount of resin to be heated in the system with 4 cm thickness is higher. In some areas, the reaction start even before that the center is

heated, as can be seen in the profile of the system at 47.5 min. It can be also observed that the glass has some insulating effect in the system. As the heating of the system continue, the center is heated and the heat generated by the material in the center is higher. The curing degree followed a similar behavior than the explained for temperature. With the time evolution, the reaction ends and the temperature decreased as explained previously. The temperature is still higher than 90 °C after 2.7 h, showing that the cooling process is slower for this system, due to the dissipation problems ascribed to the higher volume of resin.

The temporal evolution of temperature and curing degree distribution provided by the model for the epoxy–amine system cured at 150 °C is presented in Figs. 15 and 16 for the system with a thickness of 0.5 cm (Figs. 15a, 16a) and 4 cm (Figs. 15b, 16b).

In the system with 0.5 cm thickness, the heating started faster than for the system at 90 °C as a consequence of the heat in the oven is higher. The heat propagated from the

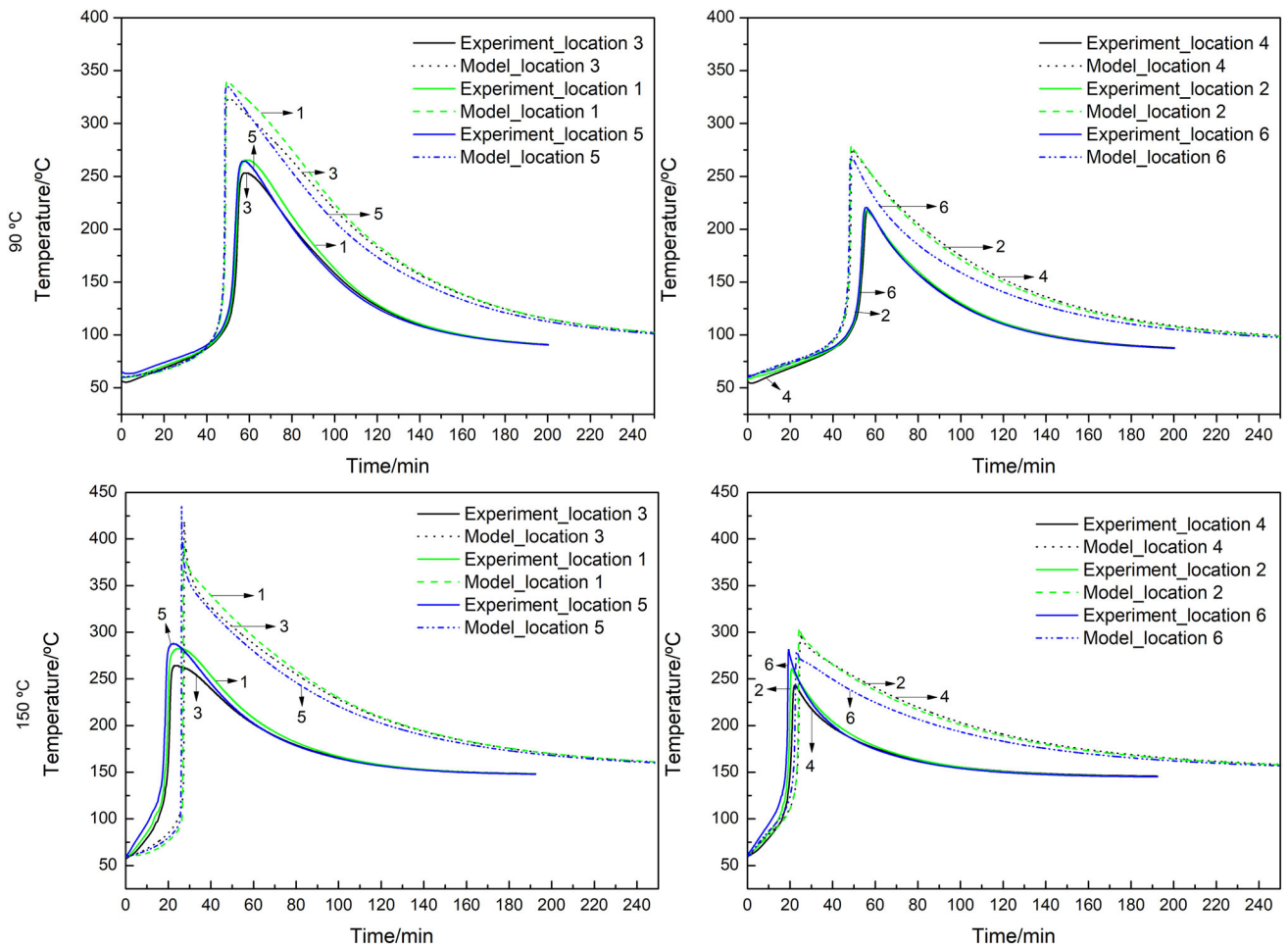


Fig. 12 Comparison of experimental and predicted temperature profiles of the DGEBA-DDM system at curing temperatures of 90 and 150 °C and at different locations in the center of the design (points 5, 1 and 3) and in the edge (points 6, 2 and 4) for the system with thickness 4 cm

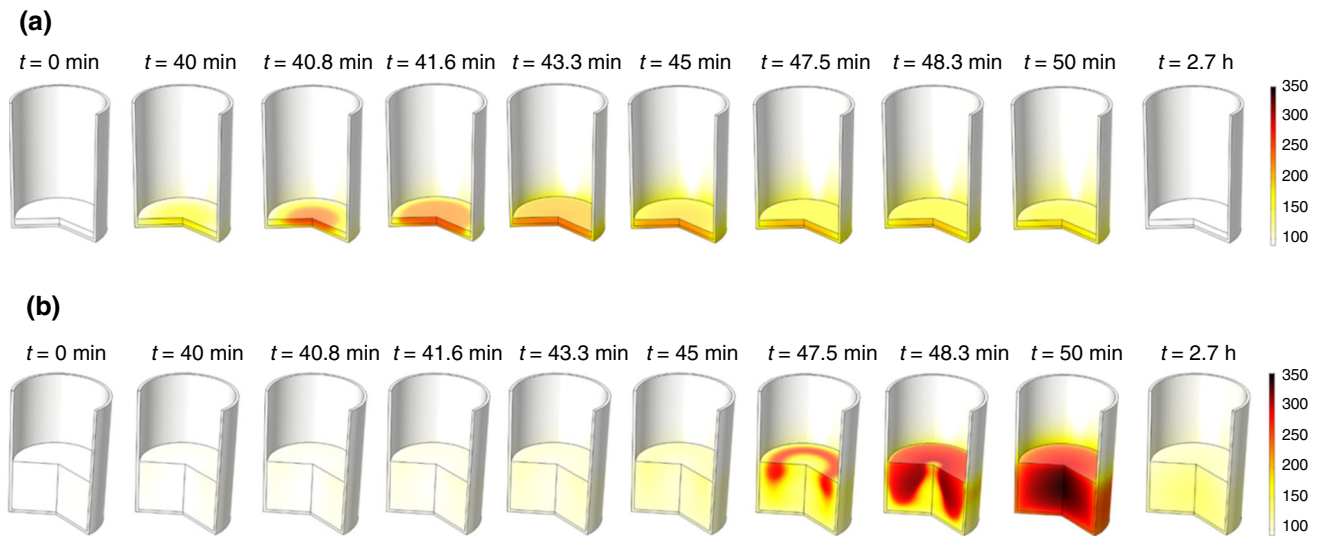


Fig. 13 Temperature distributions at different curing times in the DGEBA-DDM system at a curing temperature of 90 °C: **a** 0.5 and **b** 4 cm

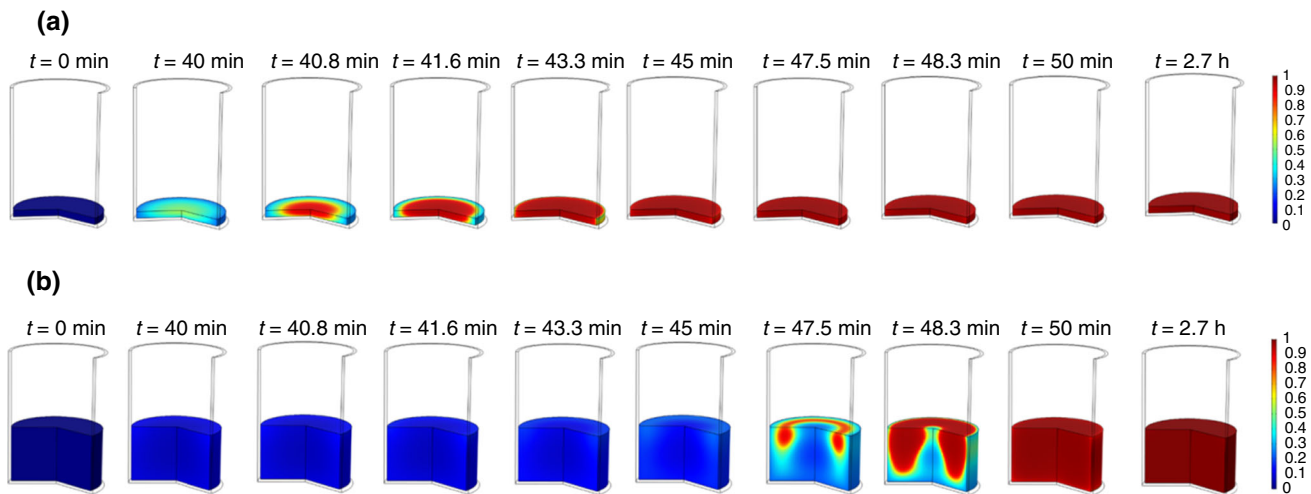


Fig. 14 Curing degree distributions at different curing times in the DGEBA–DDM system at a curing temperature of 90 °C: **a** 0.5 and **b** 4 cm

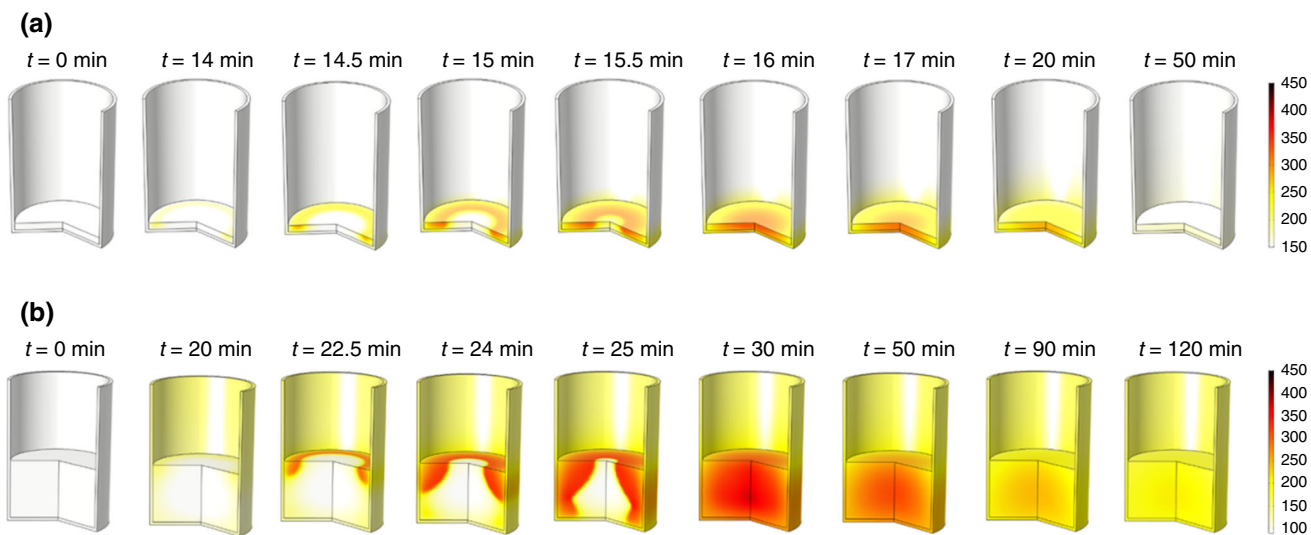


Fig. 15 Temperature distributions at different curing times in the DGEBA–DDM system at a curing temperature of 150 °C: **a** 0.5 and **b** 4 cm

external part until the center, but in some areas the reaction start even before the center is heated and the curing degree evolved fast due to the high temperature. As the heating of the system continues, the center is heated. With the time evolution, the reaction ends and the temperature decreased.

In the system with 4 cm thickness, the heating process is slower than in the system with 0.5 cm thickness due to the higher amount of resin, but faster than the process at 90 °C. The heating started to increase the resin temperature from the outer part of the glass, but due to the high curing temperature employed in the study, the reaction started faster and the temperature gradient between the outer part and the cool center is higher than 200 °C in the maximum reached. A high difference in the curing degree is also observed, being achieved a full curing in the outer part, whereas the reaction has not started in the cool center. The

insulating effect of the glass was also observed for this system. With heating, the heat generated by the material at the center is high, being reached temperatures higher than the degradation temperature of the material. As explained previously, the model overestimates the maximum temperatures and the experimental maximum peak temperature in the center of the piece for a thickness of 0.5 cm, was around 235 °C (thermocouple 1) and 283 °C for a thickness of 40 mm (thermocouple 1). However, this analysis helps to design a proper curing cycle avoiding temperatures closer to the degradation temperature of the system and avoiding significant temperature gradients inside the sample. Finally, the reaction ends and the temperature decreased in a slower way than for the system with 0.5 cm thickness.

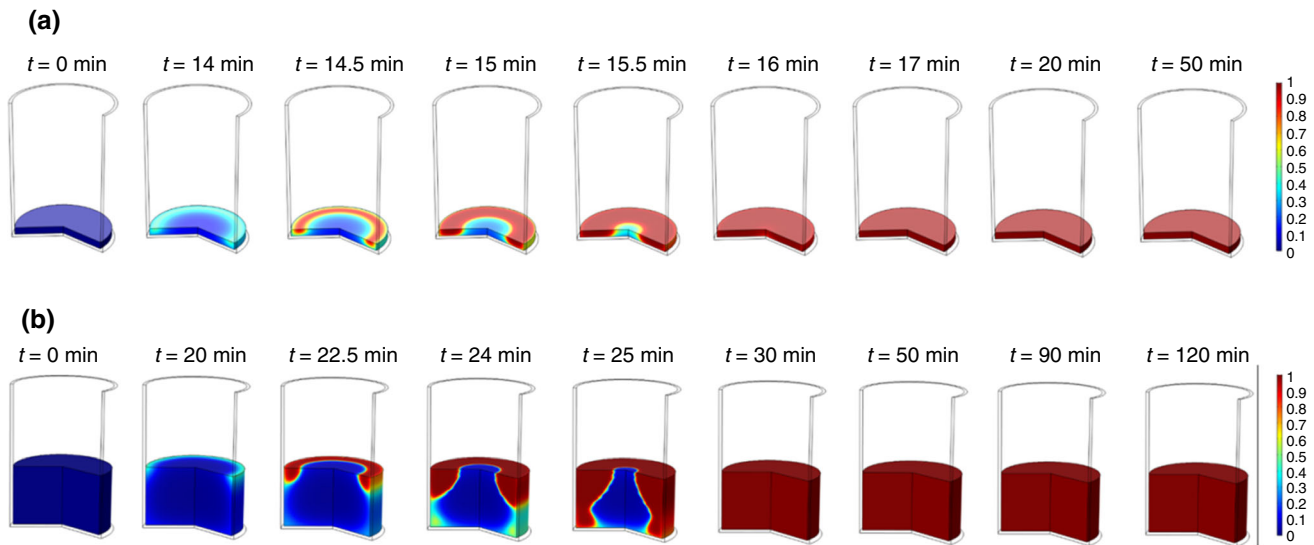


Fig. 16 Curing degree distributions at different curing times in the DGEBA- DDM system at a curing temperature of 150 °C: a 0.5 and b 4 cm

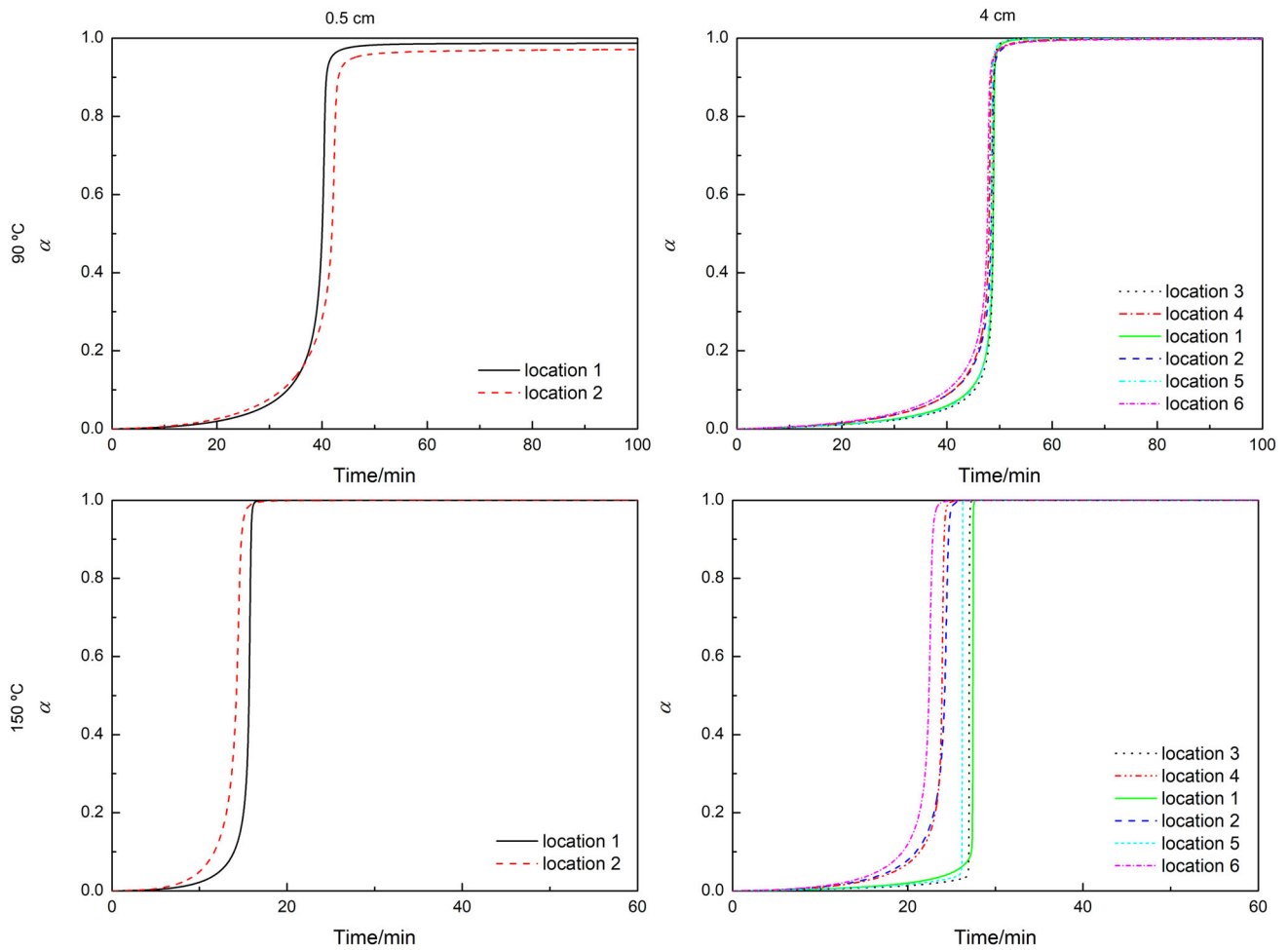


Fig. 17 Predicted curing degree profiles of the DGEBA- DDM system at curing temperatures of 90 and 150 °C for the systems with thicknesses 0.5 and 4 cm

Analyzing the evolution of the modeled curing degree for each point of the system as a function of the temperature measured by the thermocouples (Fig. 17), it can be observed the same tendency. In addition, it can be observed that the curing degree gradient in the sample is not too significant for the system cured at 90 °C, but a significant gradient is observed for the system cured at 150 °C, mainly when the thickness increases. These results demonstrated the existence of strong curing degree gradients within the pieces with high thicknesses, since different temperatures have been reached in the different locations and highlight the importance of a proper curing cycle design in order to avoid differences in crosslink densities and therefore in mechanical properties of these casting parts.

Conclusions

A thermo-kinetic model was employed to study the temperature and curing degree distribution in a DGEBA–DDM casting part during his curing process. Initially, the curing of the DGEBA–DDM system was investigated by isothermal and non-isothermal DSC. A Kamal and Sourour phenomenological model was applied to fit experimental results, but the model deviates at high levels of conversion in describing the diffusion-controlled reaction kinetics. To consider the diffusion effect, the Kamal and Sourour curing kinetics model was expanded by a diffusion model, proposed by Chern and Phoehlein. A good fitting of the experimental data was obtained with the expanded model in the analyzed range of temperatures.

A nonlinear transient heat transfer analysis combined with a curing kinetic model based on finite element procedures was developed. The model can describe the curing of the thermosetting matrix as a non-homogeneous process that takes into account the exothermal behavior of the chemical reaction. This heterogeneity is particularly developed as the thickness increases due to mass effect.

The temperature and curing degree distribution for DGEBA–DDM system during the curing process predicted by the model was compared with experimental results. Experimental data showed that the simulation procedure provides reasonable qualitative predictions, but further investigation and additional measurements are required to obtain better quantitative predictions. The results indicated that the model fits properly the heating of the sample, the time position at which the temperature starts to increase due to the heat generated during epoxy–amine reaction and also the rate at which the temperature increase, but it overestimates the maximum temperatures reached in the system as a consequence of the reaction. Nevertheless, the proposed model is shown as a powerful tool to design optimal curing cycles for thermosetting resins avoiding

temperatures closer to the degradation temperature of the system and avoiding significant temperature gradients inside the sample.

The present thermo-kinetic model provides an accurate method that allows further insight into the curing process for epoxy resin. The model is able to predict optimal curing cycles for thermosetting resins, obtaining controlled and high curing degrees. The proper curing control avoids heat degradation problems due to excess of heat, avoids temperature gradients across the system and reduces curing times without implicating the piece quality.

Acknowledgements Authors would like to acknowledge the Basque Government funding within the ELKARTEK 2015–2016 and 2016–2017 Programme, ACTIMAT. C. Monteserín wishes to thank the Iñaki Goenaga Foundation for her PhD Grant. The authors also wish to express their gratitude to the European Community's H2020 Framework Programme under Grant Agreement No. 685842 (EIROS project) and (Grupos de Investigación Gobierno Vasco, IT718-13).

References

1. Rozenberg BA. Kinetics, thermodynamics and mechanism of reactions of epoxy oligomers with amines. In: Dušek K, editor. *Advances in polymer science*. Berlin: Springer; 1985. p. 113–65.
2. Aronhime MT, Gillham JK. Time–temperature–transformation (TTT) cure diagram of thermosetting polymeric systems. In: Dušek K, editor. *Epoxy resins and composites III*. Berlin: Springer; 1986. p. 83–113.
3. Joshi SC, Liu XL, Lam YC. A numerical approach to the modeling of polymer curing in fibre-reinforced composites. *Compos Sci Technol*. 1999;59:1003–13.
4. Dai F. *Residual stresses in composite materials*. Amsterdam: Elsevier; 2014. p. 311–49.
5. Choi JH, Lee DG. Expert cure system for the carbon fiber epoxy composite materials. *J Compos Mater*. 1995;29:1181–200.
6. White SR, Hahn HT. Cure cycle optimization for the reduction of processing-induced residual stresses in composite materials. *J Compos Mater*. 1993;27:1352–78.
7. Joseph B, Hanratty FW, Kardos JL. Model based control of voids and product thickness during autoclave curing of carbon/epoxy composite laminates. *J Compos Mater*. 1995;29:1000–24.
8. Poodts E, Minak G, Mazzocchetti L, Giorgini L. Fabrication, process simulation and testing of a thick CFRP component using the RTM process. *Compos Part B Eng*. 2014;56:673–80.
9. Barkoula NM, Alcock B, Cabrera NO, Peijs T. Fatigue properties of highly oriented polypropylene tapes and all-polypropylene composites. *Polym Polym Compos*. 2008;16:101–13.
10. Zhang J. Effect of cure cycle on curing process and hardness for epoxy resin. *Express Polym Lett*. 2009;3:534–41.
11. Lin Liu X, Crouch I, Lam Y. Simulation of heat transfer and cure in pultrusion with a general-purpose finite element package. *Compos Sci Technol*. 2000;60:857–64.
12. Park HC, Goo NS, Min KJ, Yoon KJ. Three-dimensional cure simulation of composite structures by the finite element method. *Compos Struct*. 2003;62:51–7.
13. Rabearison N, Jochum C, Grandidier JC. A FEM coupling model for properties prediction during the curing of an epoxy matrix. *Comput Mater Sci*. 2009;45:715–24.
14. Oh JH, Lee DG. Cure cycle for thick glass/epoxy composite laminates. *J Compos Mater*. 2002;36:19–45.

15. Rouison D, Sain M, Couturier M. Resin transfer molding of natural fiber reinforced composites: cure simulation. *Compos Sci Technol.* 2004;64:629–44.
16. Laza JM, Vilas JL, Garay MT, Rodríguez M, León LM. Dynamic mechanical properties of epoxy–phenolic mixtures. *J Polym Sci, Part B: Polym Phys.* 2005;43:1548–55.
17. Laza JM, Julian CA, Larrauri E, Rodríguez M, Leon LM. Thermal scanning rheometer analysis of curing kinetic of an epoxy resin: 2. An amine as curing agent. *Polymer.* 1999;40:35–45.
18. Schawe JEK, Hütter T, Heitz C, Alig I, Lellinger D. Stochastic temperature modulation: a new technique in temperature-modulated DSC. *Thermochim Acta.* 2006;446:147–55.
19. Wan J, Li C, Bu Z-Y, Xu C-J, Li B-G, Fan H. A comparative study of epoxy resin cured with a linear diamine and a branched polyamine. *Chem Eng J.* 2012;188:160–72.
20. Hardis R, Jessop JLP, Peters FE, Kessler MR. Cure kinetics characterization and monitoring of an epoxy resin using DSC, Raman spectroscopy, and DEA. *Compos Part A Appl Sci Manuf.* 2013;49:100–8.
21. Wise CW, Cook WD, Goodwin AA. Chemico-diffusion kinetics of model epoxy–amine resins. *Polymer.* 1997;38:3251–61.
22. Thomas R, Durix S, Sinturel C, Omonov T, Goossens S, Groeninckx G, et al. Cure kinetics, morphology and miscibility of modified DGEBA-based epoxy resin—effects of a liquid rubber inclusion. *Polymer.* 2007;48:1695–710.
23. Borchardt HJ, Daniels F. The application of differential thermal analysis to the study of reaction kinetics 1. *J Am Chem Soc.* 1957;79:41–6.
24. Kamal MR, Sourour S. Kinetics and thermal characterization of thermoset cure. *Polym Eng Sci.* 1973;13:59–64.
25. Montserrat S, Malek J. A kinetic analysis of the curing reaction of an epoxy resin. *Thermochim Acta.* 1993;228:47–60.
26. Sourour S, Kamal MR. Differential scanning calorimetry of epoxy cure: isothermal cure kinetics. *Thermochim Acta.* 1976;14:41–59.
27. Rabearison N, Jochum C, Grandidier JC. A cure kinetics, diffusion controlled and temperature dependent, identification of the Araldite LY556 epoxy. *J Mater Sci.* 2011;46:787–96.
28. Blanco M, Corcuera MA, Riccardi CC, Mondragon I. Mechanistic kinetic model of an epoxy resin cured with a mixture of amines of different functionalities. *Polymer.* 2005;46:7989–8000.
29. Larrañaga M, Martín M, Gabilondo N, Kortaberria G, Corcuera M, Riccardi C, et al. Cure kinetics of epoxy systems modified with block copolymers. *Polym Int.* 2004;53:1495–502.
30. Chern C-S, Poehlein GW. A kinetic model for curing reactions of epoxides with amines. *Polym Eng Sci.* 1987;27:788–95.
31. Fu Y-X, He Z-X, Mo D-C, Lu S-S. Thermal conductivity enhancement with different fillers for epoxy resin adhesives. *Appl Therm Eng.* 2014;66:493–8.
32. Burger N, Laachachi A, Mortazavi B, Ferriol M, Lutz M, Toni-azzo V, et al. Alignments and network of graphite fillers to improve thermal conductivity of epoxy-based composites. *Int J Heat Mass Transf.* 2015;89:505–13.
33. Devaux O, Créac'hacdec R, Cognard JY, Mathis K, Lavelle F. FE simulation of the curing behavior of the epoxy adhesive Hysol EA-9321. *Int J Adhes Adhes.* 2015;60:31–46.
34. Van Assche G. Frequency dependent heat capacity in the cure of epoxy resins. *Thermochim Acta.* 2001;377:125–30.
35. Behzad T, Sain M. Finite element modeling of polymer curing in natural fiber reinforced composites. *Compos Sci Technol.* 2007;67:1666–73.